3D Structuring of Magnetoelastomers for Anisotropic Actuation Properties

Yagmur Atescan¹ and Namiko Yamamoto² The Pennsylvania State University, University Park, PA, 16802, USA

Smart structures with actuation function are desired for aerospace applications, including morphing airfoils, deployable structures and more. While shape memory alloys and piezoelectric ceramics and polymers are currently a popular smart material options for such applications, magnetoelastomers (MEs) can be uniquely actuated with application of noncontact magnetic field. Magnetoelastomers (MEs), composite materials made of magnetic particles and soft, non-magnetic matrix, can potentially contribute to such smart structures as a light-weight, smart material option with large strain change, fast response time (milliseconds) and anisotropic actuation properties. Other than aerospace applications, MEs, as soft actuators, have been investigated for flexible electronics, soft robotics, and biomedical applications. Anisotropic actuation properties of MEs can be controlled with particle organization within the elastomer. To provide this control, parametric studies on fabrication of MEs need to be performed. This study presents experimental work on nanoparticle organization within MEs using uniaxial, biaxial and triaxial magnetic fields and on the structure-property relationships of MEs. Iron oxide nanoparticle were used as a model nanofillers, and their surfaces were treated with silane coupling agent to improve dispersion and suspension within a polydimethylsiloxane (PDMS) elastomer. The fabricated MEs were inspected using microCT, and their anisotropic susceptibilities are being measured.

I. Introduction

Magnetoelastomers (MEs) are composite materials consisting of magnetically responsive particles (nano to micro size) distributed or organized within a non-magnetic elastomer matrix [1, 2]. Upon application of external magnetic fields, the magnetic dipoles of the particles rotate along the direction of the applied fields, resulting in physical strains: magnetostriction [3, 4]. These magnetostrictive properties of MEs can provide functions to design advanced actuators. In a very similar manner, external loadings can alter the magnetic dipole arrangement, resulting in changes to the electric, magnetic, and rheological properties of MEs; thus, MEs can also be used for sensing and vibration damping functions [5-8].

Actuation response of MEs can be tuned by structuring the magnetic particles within the elastomer [9-15]. The distribution of magnetic particles inside the elastomer can be either homogeneous or arranged. In the absence of external magnetic field during the elastomer crosslinking process, magnetic particles dispersed randomly and produce an isotropic ME. In the presence of applied magnetic field, the magnetic particle structures within the elastomer depends on combination of magnetic fields applied from different directions (uniaxial, biaxial or triaxial) [11-13, 15]. The magnetostrictive properties of MEs have been tailored through organization of microparticles in the past [4, 10]. Advanced tailoring of microparticles to achieve chain-like, sheet-like, and honeycomb-like 3D structures has been conducted by applying triaxial fields with heterodyning to particle-dispersed polymer matrices prior to cure [10, 13]. Magnetostrictive stresses and strains, which are dependent upon the magnetic susceptibility, are greater in the direction of the aligned particles due to stronger inter-particle interactions. In the past, when the anisotropic magnetostrictive properties of MEs have been characterized, the susceptibility enhancement was observed to be greater than the theoretical expectation [13]. To fully take advantage of MEs based on this positive result, a better understanding about the relationship between the particle structures and resulting magnetostrictive properties is necessary, in addition to more precise particle organization and its characterization.

In this work, a novel method is studied to magnetically organize nano-sized particles within an elastomer. A scalable fabrication of MEs with more precisely tailored particle structures using particle surface treatment and application of triaxial magnetic fields is performed. Frequency, particularly in the low range (0-1 Hz), and phase differences are used on applied magnetic fields to change the particle organization within MEs. The structure-property

¹ Graduate Research Assistant, Aerospace Engineering, 229 Hammond, University Park, PA, 16802, Student Member.

² Assistant Professor, Aerospace Engineering, 232A Hammond, University Park, PA, 16802, Senior Member.

relationships of the fabricated MEs are investigated through a detailed inspection of the particle structures using microCT scans. Magnetic nanoparticles are used, instead of microparticles, because magnetostriction is expected to become larger with decreasing particle size (< ~50 nm) due to larger interphase volume, smaller inter-particle distance, and more inter-particle contacts [16]. Instead of heterodyning, magnetic fields with lower frequency and controlled phase shift is applied to increase preciseness and tailorability of the nanoparticle structures and for energy efficiency.

II. Materials and Methods

Ferrimagnetic gamma-phase iron oxide nanoparticles (US Research Nanomaterials, US3200, γ -Fe₂O₃, ~25 nm diameter) were selected due to their high magnetic response and low remanence (66 emu/g saturation, 1226 A/m coercivity, and 1.1 emu/g remanence). Polydimethylsiloxane (PDMS, Elastomer RT 604A/B, mass ratio 9:1, 800 cP at RT) was selected as the matrix due to its relatively low viscosity, fast cure at elevated temperature and ease use.

Surface treatment of γ -Fe₂O₃ nanoparticles

First, in order to ensure dispersion and suspension, the γ-Fe₂O₃ nanoparticles were surface-treated with a silane coupling agent (Dow Corning, TMM, 3-(Trimethoxysily)propyl methacrylate) as shown in Fig. 1. The γ-Fe₂O₃ nanoparticles (8 wt%) were mixed with a combined solution of ethanol (85 wt%), DI water (5 wt%) and the TMM coupling agent (2 wt%). Mixing was conducted using a planetary ball-mill (Tencan, XQM-0.4A) for 70 hours to fragmentate the nanoparticle aggregates. To prevent re-aggregation of the nanoparticles due to heating, the ball mill was run at 300 RPM and cycled through 6 minutes clockwise, 3 minutes pause time, 6 minutes counterclockwise, and 3 minutes pause time. A mass of 14 grams of yttrium stabilized zirconia beads (0.9 mm) were used as the milling media (7:1 mass ratio of nanoparticles). Before and after this surface treatment, the γ-Fe₂O₃ nanoparticles were inspected with Fourier-transform infrared spectroscopy (FTIR, Bruker Vertex 70) at room temperature to evaluate their surface chemistry conditions (see Fig. 2). Attenuated total reflection (ATR) was conducted and verified the presence of hydroxyl groups (O-H stretch, 3600 – 3200 cm⁻¹) on the as-received γ-Fe₂O₃ nanoparticles, which are necessary to facilitate bonding with the coupling agent. The ATR spectrum also verified the presence of organic groups from the TMM coupling agent on the surface-treated γ-Fe₂O₃ nanoparticles, but this result does not necessarily indicate that bonds were formed between y-Fe₂O₃ nanoparticles and the TMM coupling agent. Thus, diffuse reflectance infrared Fourier-transform spectroscopy (DRIFTS) was also conducted at 150 °C (see Fig. 3). The elevated temperature evaporated absorbed water from the surface of the γ-Fe₂O₃ nanoparticles allowing for detection of Fe-O-H stretch. The peak associated with the Fe-O-H stretch (3700 cm⁻¹) was observed with the as-received γ-Fe₂O₃ nanoparticles but not with the surface-treated nanoparticles indicating that hydroxyl groups were consumed and thus bonding was successfully achieved. The particle aggregate sizes were measured using dynamic light scattering (DLS, Mastersizer 3000, Malvern, size range of 10 nm – 3500 μm). A laser beam passed through dispersed nanoparticle aggregates, and the angular variation of scattered light intensity was measured and analyzed to calculate the size of the nanoparticle aggregates responsible for creating the scattering pattern. For the DLS measurement, the as-received γ-Fe₂O₃ nanoparticles were ultrasonicated in DI water (0.1 vol%, room temperature, 20 min) and the surface-treated γ-Fe₂O₃ nanoparticles were ultrasonicated in ethanol (0.1 vol%, room temperature, 20 min). Measurement was repeated three times for each sample. The aggregate size was successfully decreased from ~1110 nm to ~220 nm after surface treatment (see Fig. 4) in order to decrease the gravitational sedimentation.

Fig. 1 Schematic showing surface treatment of γ -Fe₂O₃ nanoparticles with a silane coupling agent for the PDMS elastomer.

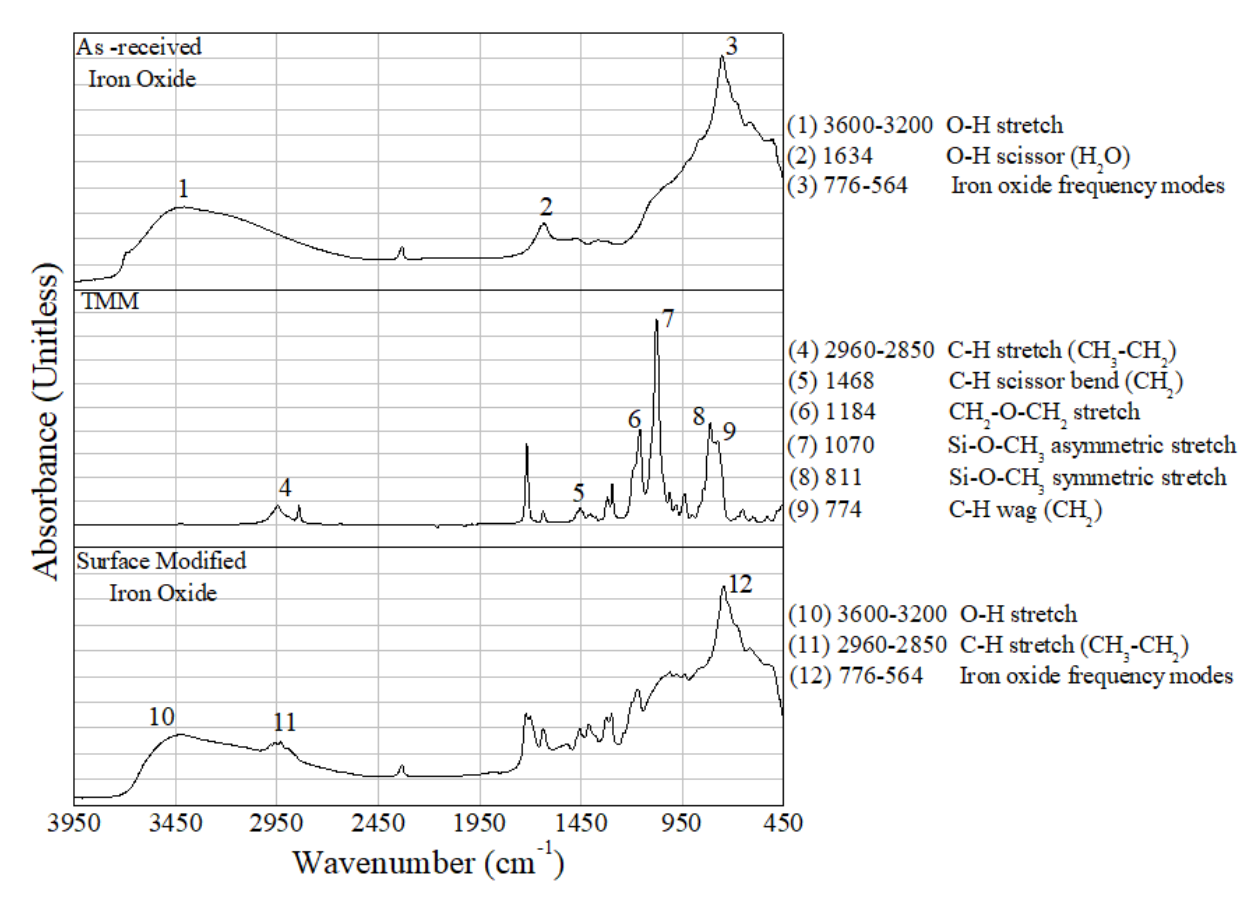


Fig. 2 FTIR (ATR) spectra for the as-received γ-Fe₂O₃ nanoparticles (top), silane coupling agent (TMM) (middle), and the surface-treated γ-Fe₂O₃ nanoparticles (bottom).

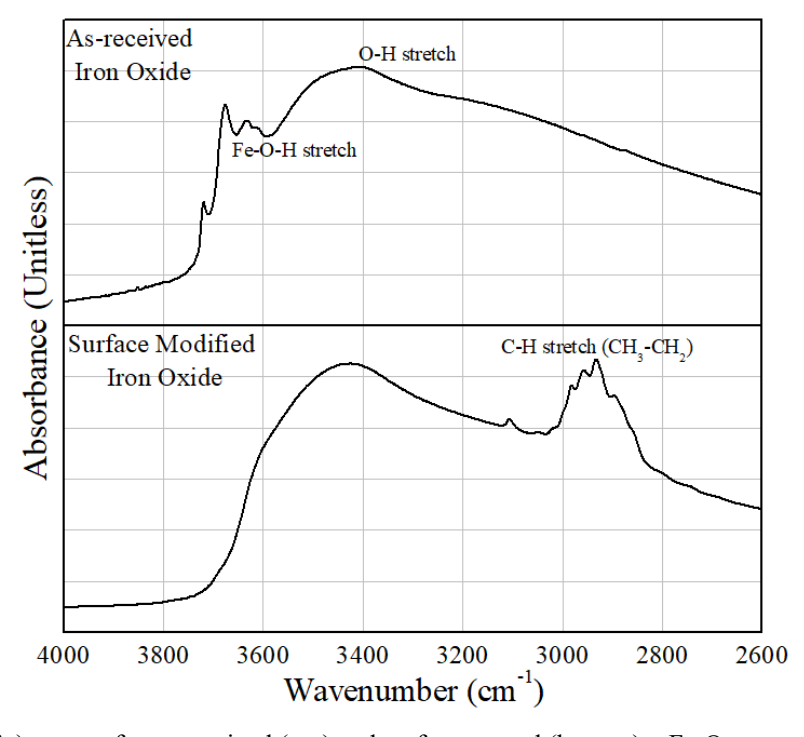


Fig. 3 FTIR (Drifts) spectra for as-received (top) and surface-treated (bottom) γ-Fe₂O₃ nanoparticles at 150 °C.

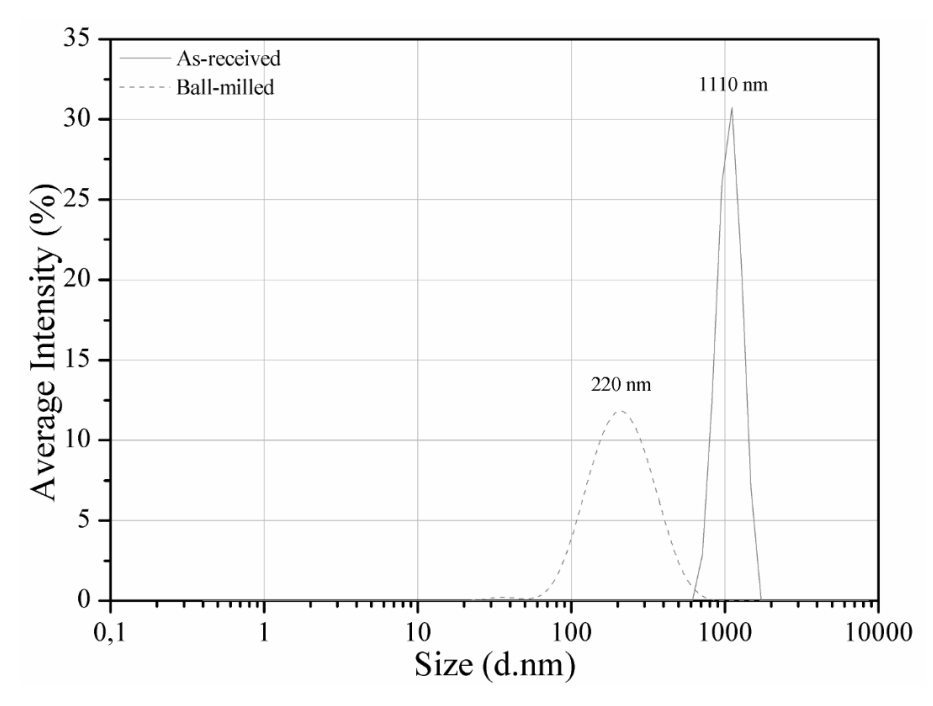


Fig. 4 Particle aggregate size distribution measured using DLS.

Magnetic assembly of MEs

Second, the surface-treated γ-Fe₂O₃ nanoparticles were centrifuged out of the solution, dispersed in the elastomer matrix (1 vol%) and structured within the elastomer using external magnetic fields. The surface-treated γ-Fe₂O₃ nanoparticles were ultrasonicated (Branson Ultrasonics, CPX-952-117R) in PDMS Part A (50 °C for 15 min) and then vacuumed at room temperature for 10 min to evaporate the remaining solvent. The mixture was further processed to ensure nanoparticle dispersion: ultrasonication (50 °C for 15 min) and centrifugal mixer (Thinky Planetary Centrifugal Mixer, ARE-310) (2000 rpm for 30 min). Then, the crosslinking agent (PDMS Part B) was added and further mixed using the centrifugal mixer (2000 rpm for 5 min). This well-dispersed mixture was poured into an aluminum mold (1.91 cm x 1.91 cm x 0.95 cm) and the mold was placed centered, and along axis, of a triaxial Helmholtz coil system. Magnetic fields were applied for 15 min, during which the mold was heated to 40°C using a heating pad (Omega, SRFG-203/10) to decrease the elastomer viscosity for effective nanoparticle assembly. After magnetic assembly was completed, the mixture was cured at 70 °C for 30 min while keeping the magnetic field application. Post-cure was conducted in an oven, without magnetic field application, at 120 °C for 2 hours. The Helmholtz set-up (Micro Magnetics, 208 VAC, 50-60 Hz, 30 A) is shown in Fig. 5 and can provide magnetic fields of varying strength (up to ± 300 G in the x-axis, ± 250 G in the y-axis, and ± 180 G in the z-axis) and frequency (0 to 1 Hz, ~ 0.1 Hz resolution, < ± 1 % gradient), with the control of phase shift (± 180 degrees). The system can apply a uniform magnetic field over the volume of 3.8 cm (x-direction) x 6.4 cm (y-direction) x 8.9 cm (z-direction). While field application was controlled by software, the field strength was verified with a gaussmeter (Lakeshore 425). The magnetic fields applied for ME fabrication are listed in Table 1.

MicroCT scan of γ-Fe₂O₃ nanoparticle structure in MEs

The magnetically assembled γ -Fe₂O₃ nanoparticle structures were characterized using microCT (GE Phoenix vtome XL). MicroCT is a nondestructive technique and can provide a complete three-dimensional map of the sample geometry [17]. During microCT scanning, attenuation of X-rays passing through the sample is measured by a detector. Rotation of the sample and remeasurement of the attenuated X-rays provides a stack of two-dimensional images and reconstruction of these images produces a three-dimensional volume. An important parameter of microCT is the voxel resolution (smallest volume element dimensions). The inspected sample size needs to be small enough in order to obtain a high resolution, but also big enough to observe the microstructure of the sample. In this study, 3 mm x 3 mm x 5 mm sized rectangular prisms were extracted from the bottom edge of the bulk sample for microCT inspection (see Fig. 6). A voxel resolution of 3 μ m x 3 μ m was obtained with a 66x magnification. The measurement parameters were set as follows: focus-to-detector distance (FDD) as 550 mm, focus-to-object distance (FOD) as 8.25 mm, and the X-ray beam acceleration voltage as 80 keV. For image processing ImageJ/Fiji software was used.

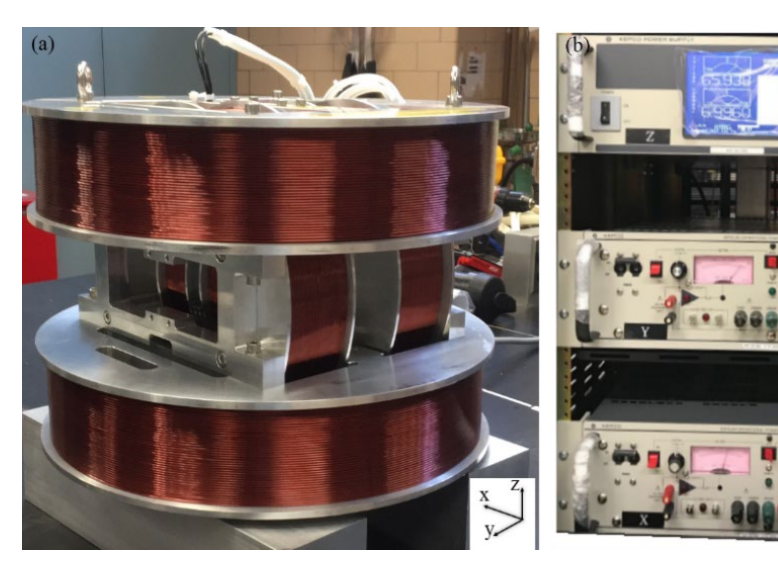


Fig. 5 Experimental set-up of (a) triaxial Helmholtz coil system, and (b) power supplies.

Table 1. Magnetic fields applied for ME fabrication.

	X-Axis			Y-Axis			Z-Axis		
Field Type	Strength	Freq.	Phase	Strength	Freq.	Phase	Strength	Freq.	Phase
	[G]	[Hz)]	[degree]	[G]	[Hz)]	[degree]	[G]	[Hz]	[degree]
Random	-	-	-	-	-	-	ı	-	-
Uniaxial	300	0	0	-	-	-	ı	-	-
Biaxial-1	250	1	0	250	1	90	ı	-	-
Biaxial-2	250	0.5	0	250	1	45	-	-	-
Biaxial-3	180	0.5	0	180	0.51	45	-	-	-
Triaxial-1	180	1	0	180	1	90	180	0	0
Triaxial-2	250	1	0	250	1	90	180	1	0
Triaxial-3	180	0.5	0	180	1	45	180	0	0

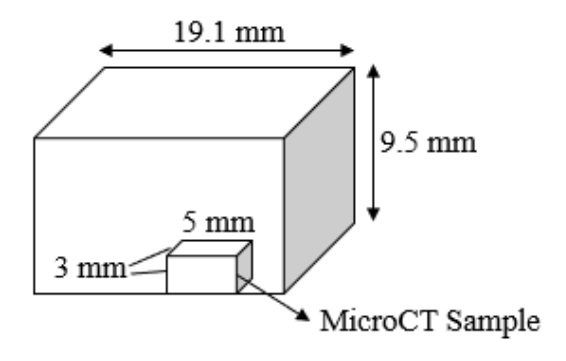


Fig. 6 MicroCT sample extraction from the fabricated ME sample.

III. Results and Discussion

Fabricated eight samples, listed in **Table 1**, were inspected with microCT and their two-dimensional views are given in **Fig. 7-14**. The effectiveness of the coupling agent is seen in the uniform dispersion of the randomly orientated surface-treated γ -Fe₂O₃ (settlement thickness is ~0.14 mm) (see **Fig. 7**). By changing the magnitude, various nanoparticle structures were demonstrated with varying frequency and phase shift of the magnetic fields. With the uniaxial field application, chain-like nanoparticle structures were observed (see **Fig. 8**). As seen from **Fig. 9**, **10** and **11**, sheet-like structures obtained with biaxial (rotating) field (constant strength and angular velocity in the x-y plane) application; magnetic field rotation enhanced transverse assembly of the nanoparticles within the x-y plane. Frequency and phase differences provided longer assembly in x-direction for Biaxial-2 sample than for Biaxial-1 sample (see

Fig. 9-10). Small (0.01 Hz) frequency difference between x and y direction fields caused directional orientation of particles within sheet structures (see **Fig. 11**). With combination of the rotating field within the x-y plane and a static field in the z-direction Triaxial-1 sample was fabricated. Due to the same field strength in all three directions and static application of field in z-direction, vertical chain structures were obtained (see **Fig. 12**). To provide a three-directional organization of particles field strength on x and y directions were increased and oscillating field was applied in z direction (Triaxial-2 sample, **Fig. 13**). With the effect of rotating field on x-y plane and unsteady z-direction field strength, angled sheet-like structures were observed (see **Fig. 13**). Differently from Triaxial-1 sample, in Triaxial-3 sample, x-direction frequency was decreased to 0.5 Hz and phase difference between x and y directions was decreased to 45 degree. While chain structures in z-direction were still observed, smaller frequency in x-direction caused assemblies in this direction as well. As a result of that, thicker chain structures were seen on Triaxial-3 sample (**Fig. 14**). Further analysis will be performed to provide a detailed information about applied magnetic field—nanoparticle assembly relation.

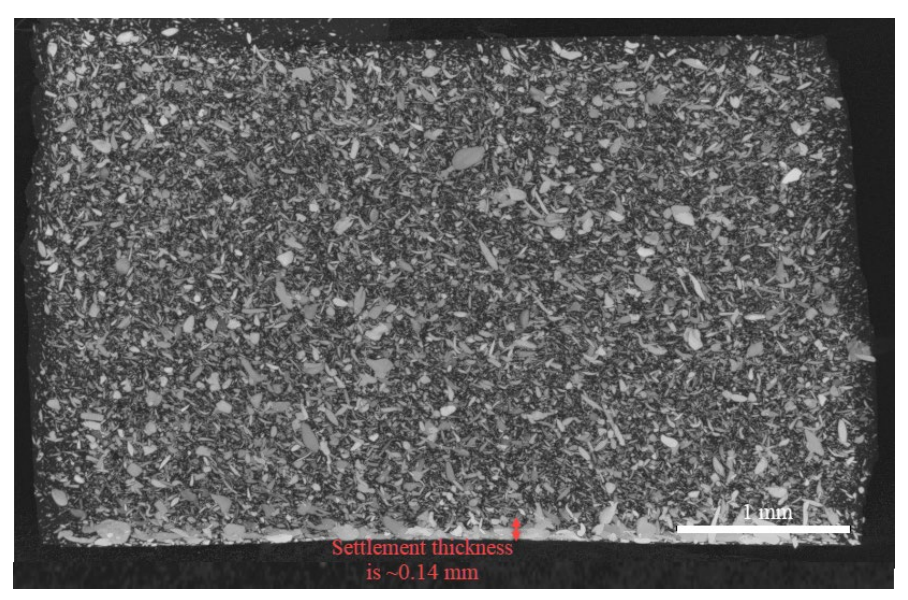


Fig. 7 MicroCT scan of ME with random particle organization.

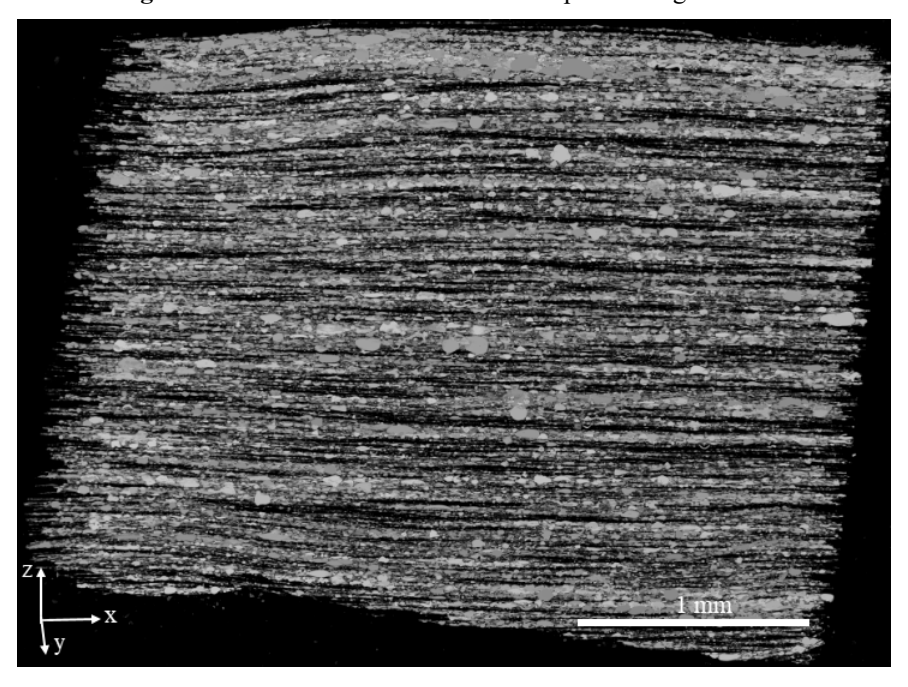


Fig. 8 MicroCT scan of ME assembled using the Uniaxial field.

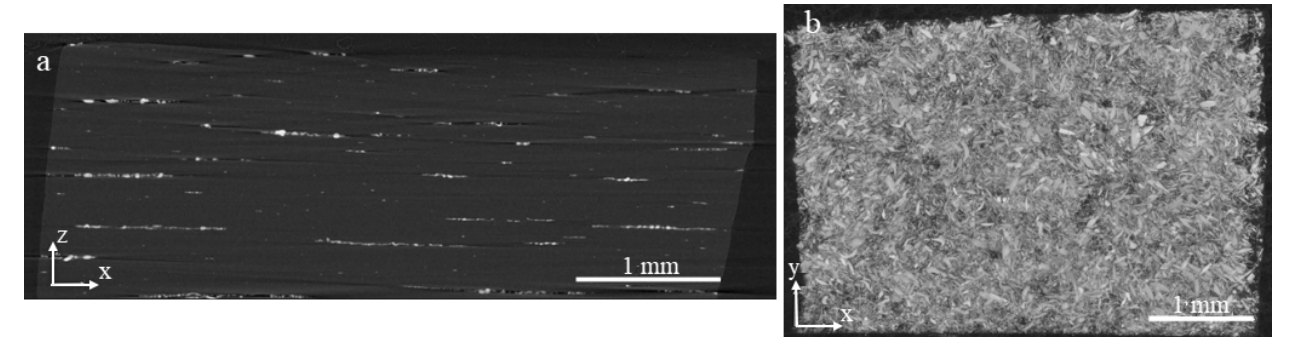


Fig. 9 MicroCT scan of ME assembled using the Biaxial-1 field (a) side view, (b) top view.

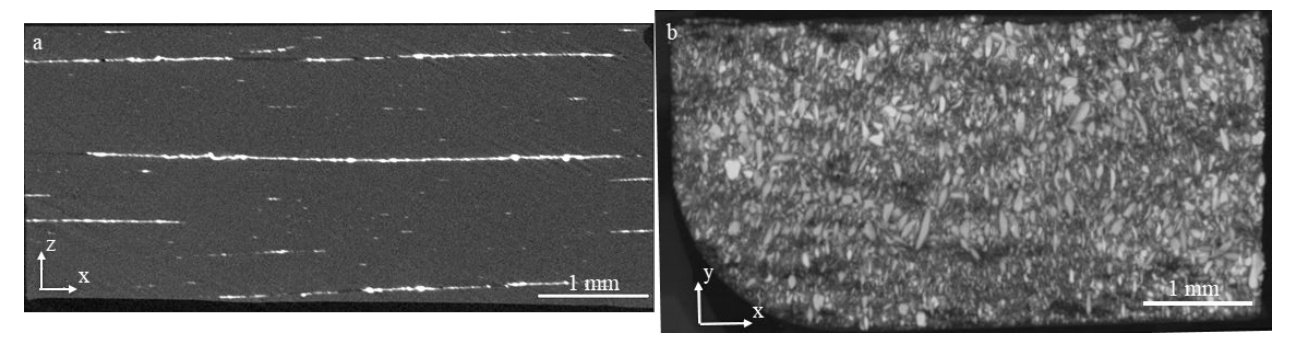


Fig. 10 MicroCT scan of ME assembled using the Biaxial-2 field (a) side view, (b) top view.

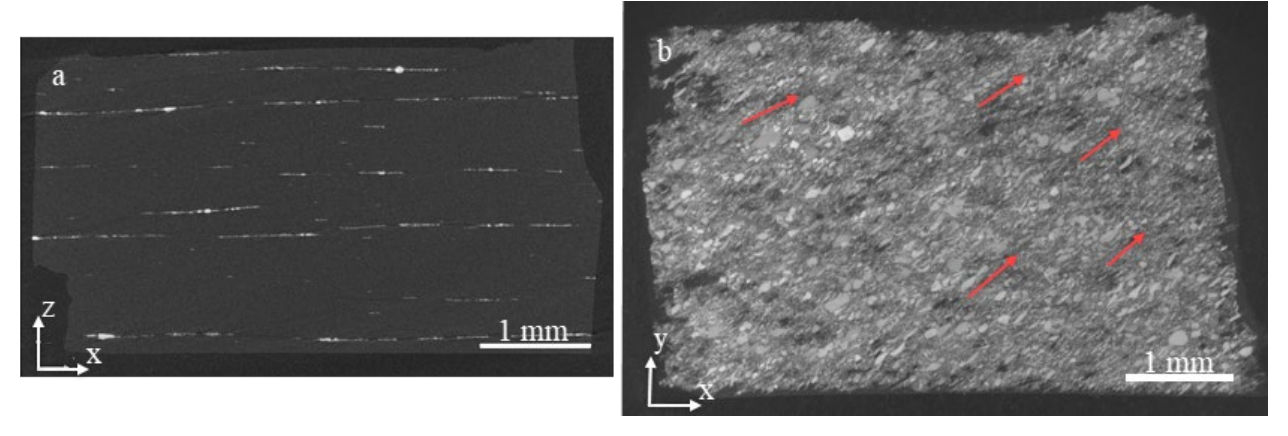


Fig. 11 MicroCT scan of ME assembled using the Biaxial-3 field (a) side view, (b) top view.

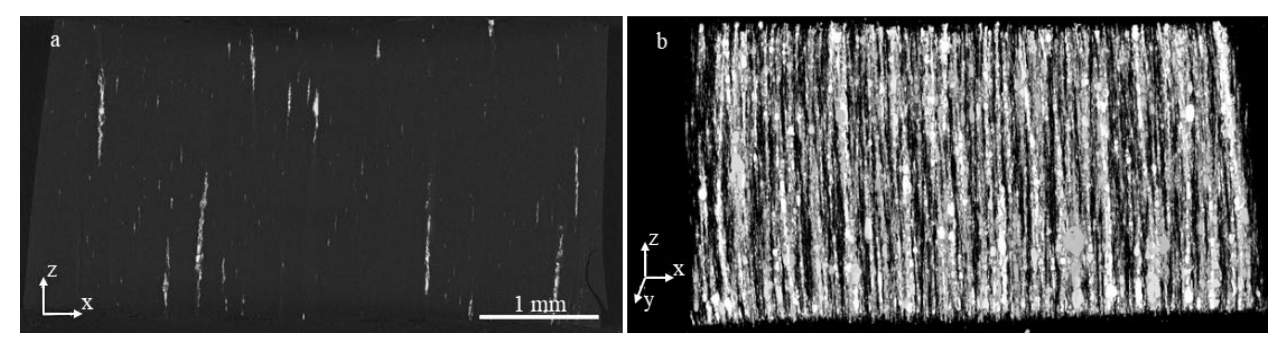


Fig. 12 MicroCT scan of ME assembled using the Triaxial-1 field (a) side view, (b) 3D projection.

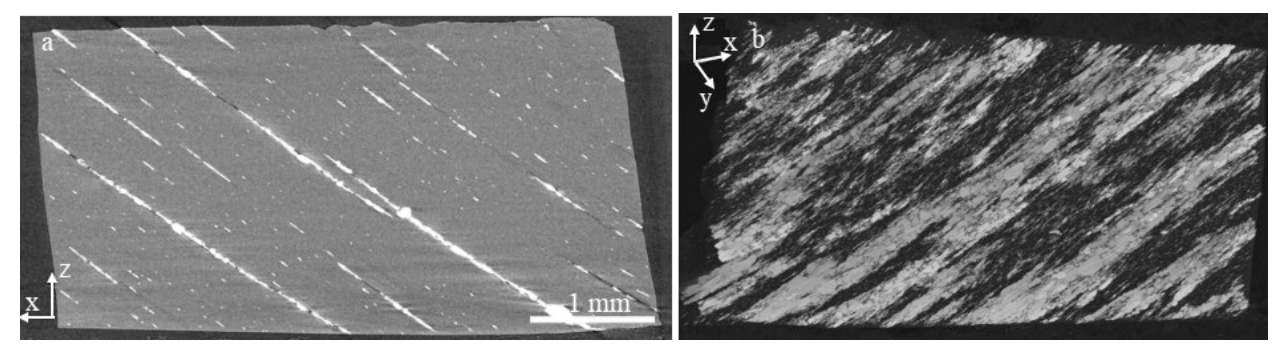


Fig. 13 MicroCT scan of ME assembled using the Triaxials-2 field (a) side view, (b) 3D projection.

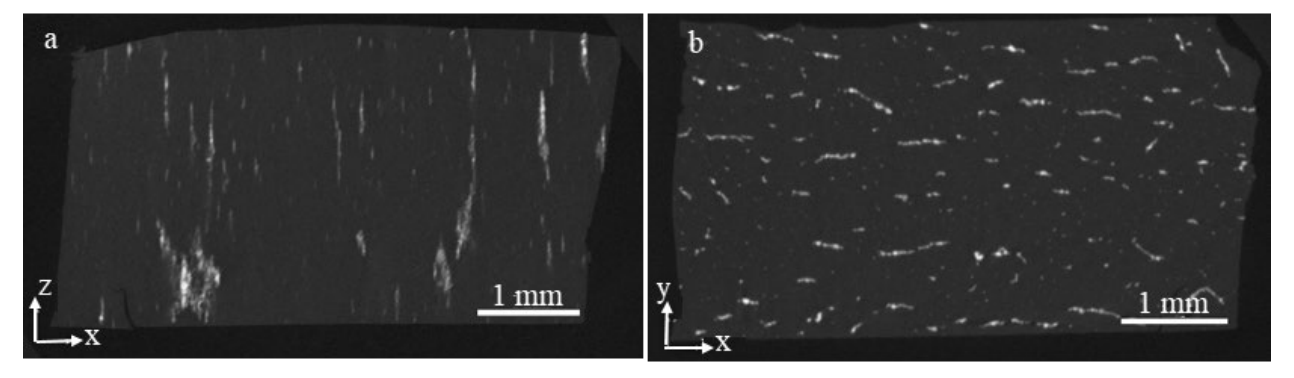


Fig. 14 MicroCT scan of ME assembled using the Triaxials-3 field (a) side view, (b) top view.

IV. Conclusion

The goal of this study is to better understand the organization characteristics of γ -Fe₂O₃ nanoparticles exposed to multidirectional magnetic fields, which will enable scalable fabrication of tailored nanocomposites. The dispersion of the nanoparticles within the elastomer matrix is important to ensure continuous and uniform material response. A uniform dispersion was obtained by surface treatment of γ -Fe₂O₃ nanoparticles with silane coupling agent, TMM. Magnetic organization of a low volume fraction γ -Fe₂O₃ nanoparticles within a high viscosity elastomer matrix was achieved. The frequency, particularly in the low range (0-1 Hz), and phase differences were confirmed to be the effective parameter to determine the particle organization characteristics. Effective control of nanoparticles with low frequencies requires less power and is thus advantageous. MicroCT scans of ME samples were provided to better understand the structuring differences between the different magnetic field combinations.

Future work will include additional studies on triaxial magnetic field assembly of particles. More quantitative information about these assemblies will be obtained by processing the microCT data, by combining image processing filters available in ImageJ/Fiji software package and through automated voxel classification (fiber, matrix, or pore) with in-house JAVA/Python-based learning algorithm (FastRandomForest) [18]. Effects of anisotropic particle structures on magnetic susceptibility of MEs will be investigated using Vibrating Sample Magnetometer (VSM). Anisotropic actuation properties of the fabricated magnetoelastomers will be defined with magnetostriction measurements. The evaluated nanoparticle structure and magnetic properties of MEs will be compared and verified with analytical studies.

Acknowledgements

This material is based upon work supported by the National Science Foundation under Grant No. 1844670, and by the Office of Naval Research, Grant No. N00014161217. The authors would also like to thank Tim Stecko of the Quantitative Imaging Laboratory at Pennsylvania State University for his assistance with the microCT measurements.

References

- 1. Ahamed, R., S.B. Choi, and M.M. Ferdaus, *A state of art on magneto-rheological materials and their potential applications*. Journal of Intelligent Material Systems and Structures, 2018. **29**(10): p. 2051-2095.
- 2. C. Ruddy, E.A.a.G.B., *A review of magnetorheological elastomers: properties and application.* 2012: Advanced Manufacturing Science Research Centre, Mechanical Engineering, University College Dublin, Belfield, Dublin 4, Ireland. p. 1-7.
- 3. Han, Y., et al., *Magnetostriction and Field Stiffening of Magneto-Active Elastomers*. International Journal of Applied Mechanics, 2015. 7(1).
- 4. James E. Martin, R.A.A., Douglas Read, Gerald Gulley, *Magnetostriction of field-structured magnetoelastomers*. Physical Review E, 2006. **74**(051507).
- 5. Kallio, M., T. Lindroos, and S. Aalto, *The elastic and damping properties of magnetorheological elastomers*. Applied Material Research at Vtt, 2006: p. 110-+.
- 6. Liao, G.J., et al., *The design of an active-adaptive tuned vibration absorber based on magnetorheological elastomer and its vibration attenuation performance.* Smart Materials & Structures, 2011. **20**(7).
- 7. Chen, L., et al., *Investigation on magnetorheological elastomers based on natural rubber*. Journal of Materials Science, 2007. **42**(14): p. 5483-5489.
- 8. Chen, L., X.L. Gong, and W.H. Li, *Microstructures and viscoelastic properties of anisotropic magnetorheological elastomers*. Smart Materials & Structures, 2007. **16**(6): p. 2645-2650.
- 9. Jolly, M.R., J.D. Carlson, and B.C. Munoz, *A model of the behaviour of magnetorheological materials*. Smart Materials & Structures, 1996. **5**(5): p. 607-614.
- 10. Martin, J.E., *Using triaxial magnetic fields to create optimal particle composites*. Composites Part a-Applied Science and Manufacturing, 2005. **36**(4): p. 545-548.
- 11. Martin, J.E., R.A. Anderson, and C.P. Tigges, *Simulation of the athermal coarsening of composites structured by a biaxial field.* Journal of Chemical Physics, 1998. **108**(18): p. 7887-7900.
- 12. Martin, J.E., R.A. Anderson, and C.P. Tigges, *Simulation of the athermal coarsening of composites structured by a uniaxial field.* Journal of Chemical Physics, 1998. **108**(9): p. 3765-3787.
- 13. Martin, J.E., et al., *Using triaxial magnetic fields to create high susceptibility particle composites.* Physical Review E, 2004. **69**(2).
- 14. Martin, J.E., et al., *Anisotropic magnetism in field-structured composites*. Physical Review E, 2000. **61**(3): p. 2818-2830.
- 15. Puente-Cordova, J.G., et al., Fabrication and Characterization of Isotropic and Anisotropic Magnetorheological Elastomers, Based on Silicone Rubber and Carbonyl Iron Microparticles. Polymers, 2018. **10**(12).
- 16. FL, B.R., Multifunctional Polymer Nanocomposites. 2010, CRC Press.
- 17. Gunther, D., et al., *X-ray micro-tomographic characterization of field-structured magnetorheological elastomers*. Smart Materials and Structures, 2012. **21**(1).
- 18. Madra, A., N. El Hajj, and M. Benzeggagh, *X-ray microtomography applications for quantitative and qualitative analysis of porosity in woven glass fiber reinforced thermoplastic*. Composites Science and Technology, 2014. **95**: p. 50-58.